Electronic Supplementary Material (ESI) for Environmental Science: Nano.
This journal is © The Royal Society of Chemistry 2021

Supplementary Information

Developing physicochemical property-based ecotoxicity characterization factors for silver nanoparticles under mesocosm conditions for use in life cycle assessment

Sila Temizel-Sekeryan[a], Andrea L. Hicks[a,*]

[a] Department of Civil and Environmental Engineering, University of Wisconsin-Madison, Madison, WI 53706, USA

[*] Corresponding author: hicks5@wisc.edu, 2208 Engineering Hall, 1415 Engineering Drive, Madison, WI 53706, USA

2 figures, 9 tables, 24 pages

List of Figures

List of Tables

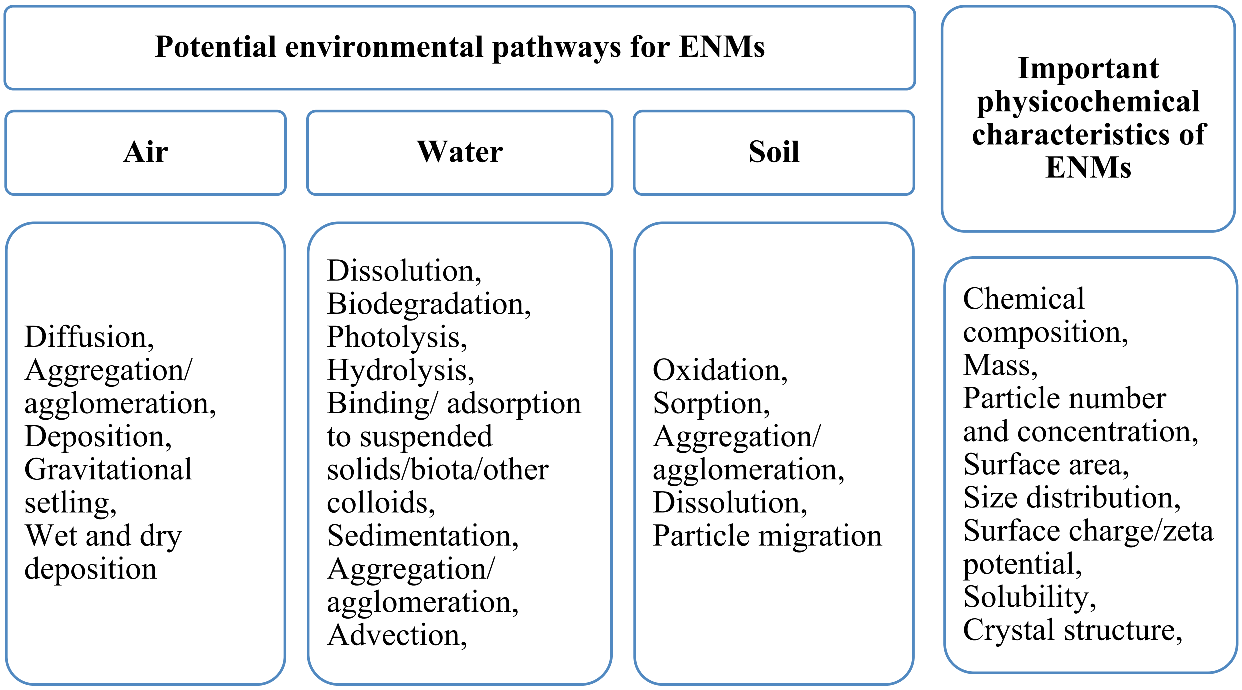

Figure S1. Potential environmental pathways for nanomaterials and physicochemical characteristics of ENMs that affect fate factors (Baun et al., 2017; Lamon et al., 2019; Miseljic and Olsen, 2014; Rosenbaum et al., 2008; Tortella et al., 2020)

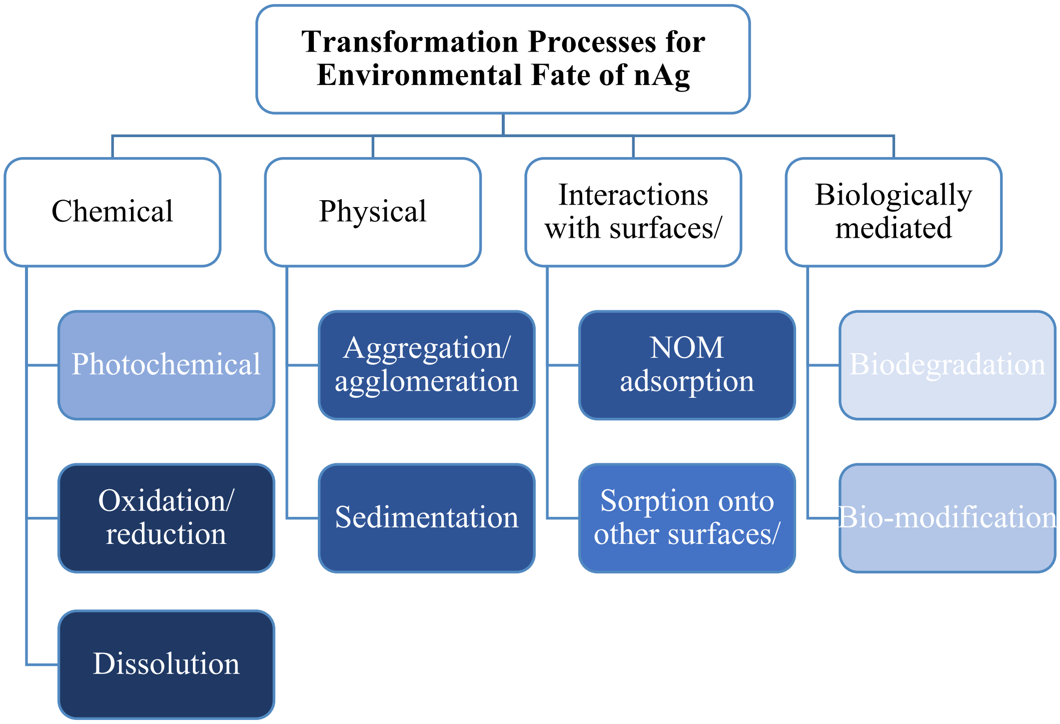

Figure S2. Relative importance of potential transformation processes in modeling environmental fate of nAg (darker shades indicate higher importance) (Baun et al., 2017; Hartmann et al., 2014)

As the current paper aims to develop freshwater ecotoxicity CF for nAg, studies that define fate and behavior of nAg are reviewed and factors affecting the fate of nAg are listed.(Baun et al., 2017; Dale et al., 2013; Furtado et al., 2015; Hartmann et al., 2014; Levard et al., 2012; Maiga et al., 2020; Peng et al., 2017; Tortella et al., 2020) Figure S2 shows the processes that are relevant to nAg and illustrates the relative importance of these processes using a color scheme.(Baun et al., 2017) Throughout the literature, it was found that nAg go through several transformation processes depending on their physicochemical characteristics as well as the properties of the release media with dissolution, oxidation/reduction and aggregation/agglomeration being the most dominant ones among others. Hartmann et al. argued that as nAg are unstable in the presence of light, photochemical transformation process may be neglected. Also, as being an inorganic ENM, the biodegradation of nAg is not expected to be as relevant as the previously mentioned processes.(Hartmann et al., 2014) Peng et al. and Peijnenburg et al. provided comprehensive assessments on each of the potential environmental transformation process and the impacts of different conditions on those processes.(Peijnenburg et al., 2015; Peng et al., 2017) For instance, after explicitly defining the dynamics of aggregation of metallic ENMs, effects of size, shape, surface coating, pH, ionic strength and presence of organic matter on aggregation are elaborated in detail.(Peijnenburg et al., 2015; Peng et al., 2017; Quik et al., 2011)

Review of characterization factor literature for nAg

In order to explore the previous studies that calculated CFs for nAg, a literature survey is conducted by using an academic search engine, Web of Science Core Collection, by searching combinations of key terms including characterization factors, nanomaterial, nanosilver and nanosilver-enabled. From this search, three studies were identified where CFs are derived for nAg.(Garvey et al., 2019; Miseljic and Olsen, 2014; Pu, 2017) Table S1, yellow shaded cells, present a summary of these studies along with the calculated/assumed FF, XF and EF, and derived CFs.

As being the first CF study for nAg, Miseljic and Olsen used simplifying assumptions to estimate the freshwater ecotoxicity potential of nAg. They suggested that nAg will have a short substance residence time in freshwater (i.e. rapid transformation, aggregation and sedimentation time), which resulted in an FF of 1.(Miseljic and Olsen, 2014) They also assumed that the exposure is equal to the environmental concentration of nAg, and therefore neglected the XF. For EF, Miseljic and Olsen compiled in total of 21 EC_{50} values for three trophic levels (algae, crustacean and fish) and calculated the EF as 8,576 PAF.m^3/kg.(Miseljic and Olsen, 2014) Another study by Pu developed a fate model which involves calculating the FF from rate constants of certain transformation processes, such as advection, dissolution, sedimentation.(Pu, 2017) For EF, Pu compiled toxicity data for three trophic levels (algae, crustacean and fish) and calculated the EF as 14,502 PAF.m^3/kg. They argued that given that the XF calculation based on USEtox involves partitioning coefficients and they are not representative for ENMs, an *ultra-conservative* XF needs to be assumed which is equal to considering 100% bioavailability.(Pu, 2017) Lastly, Garvey et al. used an adapted version of USEtox model, where they computed *realistic-* and *worst-*case scenarios. They calculated the FF using substance specific partitioning coefficients as USEtox recommended. In order to calculate the EF, Garvey et al. used in total of 73 different toxicity data (including EC_{50}, IC_{50} and LC_{50}) for four phyla (Arthropoda, Chordata, Chlorophyta and Heterokontophyla) and calculated EF with a range of 13,497 – 281,144 PAF.m^3/kg. For XF, they used statistical simulations since empirically determined exposure factors were not available in the literature, and suggested that nAg is 60-80% bioavailable.(Garvey et al., 2019)

As previously mentioned, the XF and FF depend on the physicochemical properties of nAg and the conditions of the release media.(Lamon et al., 2019; Westerhoff and Nowack, 2013) Additionally, different size and coating of nAg have a significant impact on EF.(Temizel-Sekeryan and Hicks, 2020) These factors are needed to be considered while developing nAg specific CFs. Overall, previous studies that derive nAg-CFs used various approaches and did not take into account the external (i.e. media dependent) and internal (i.e. ENM dependent) factors, which are critically important.

Table S1. Parameters for fate factor calculation extracted from a mesocosm studies (Espinasse et al., 2018; Geitner et al., 2019, 2017; Stegemeier et al., 2017).

Parameter	**Symbol**	**Unit**	**Value (Range)**
pH	pH	-	7-10
Conductivity	S	µS/cm	111 ± 20
Radius of nAg	r_{nAg}	nm	24.65 (PVP-nAg)
Diameter of nAg (DLS)	d_{nAg}	nm	49.3 (PVP-nAg)
Radius of SPM	r_{SPM}	µm	0.75
Diameter of SPM	d_{SPM}	µm	1.5 ± 12
Density of nAg	ρ_{nAg}	kg/m^3	10,500
Mass concentration of SPM	$C_{mass, SPM}$	mg/l	80 ± 12
Aggregation efficiency	$\alpha_{het-agg}$	-	0.012
Depth of water	h_w	m	1.2
Volume of water	V_w	m^3	3.56 (H/W/D 0.81/3.66/1.2)
Area of freshwater	$A_{freshwater}$	m^2	2.97
Area of soil	A_{soil}	m^2	0.732
Water temperature	T_{water}	K	295
Dynamic viscosity of water	μ_{water}	Ns/m^2	0.000958 (22^{o}C)*
Initial concentration of nAg	C_0	ppm	10
Dissolved nAg at time t (2 days)	C_{ions}	ppm	0.53

* calculated based on the formula of $\mu_{water} = (2.414 * 10^{-5}) * 10^{247.8/(T-140)}$

Table S2. Remaining parameters for fate factor calculation that are not available in mesocosms (bold values are used in calculation)

Parameter	**Symbol**	**Unit**	**Value (Range)**	**Reference**
Density of water	ρ_{water}	kg/m^3	1000	(Fantke et al., 2017)
Boltzmann constant	k_B	J/K	1.38E-23	(Deng et al., 2017a; Pu, 2017)
Surface water shear rate	G	s^{-1}	10	(Meesters et al., 2014)
Gravitational acceleration on earth	g	m/s^2	9.81	(Fantke et al., 2017)
Precipitation rate	$k_{precipitation}$	mm/yr	710 (for US)	(Kounina et al., 2014)
Density of SPM	ρ_{SPM}	kg/m^3	**1570**	*averaged value*
			2000[a] 1230[b] 1100 – 2500[c] 1250 (1100 – 2000)[d]	a (Salieri et al., 2015) b (Pu, 2017) c (Praetorius et al., 2012) d (Quik, 2013)
Water run-off fraction	φ	%	37 (for US)	(Kounina et al., 2014)

Table S3. Considerations for calculating the freshwater ecotoxicity characterization factors for ENMs (listed in alphabetical order based on references, shaded cells represent nAg)

ENM	**Considered processes for fate modeling**	**FF (days)**	**XF (%)**	**EF (PAF.m³/kg)**	**CF (PAF.m³.day/kg or CTUe/kg)**	**Reference**
CNT	Sedimentation (k_{sed}= 6.8 × 10^{-10} s^{-1}) Heteroaggregation ($k_{hetero\text{-}agg}$= 6.9 × 10^{-11} s^{-1}) Advection (k_{adv}= 6.91 × 10^{-9} s^{-1})	1509	81.1	55.4	6.78+04	(Deng et al., 2017a)
GO	Sedimentation (k_{sed}= 2.5 × 10^{-8} s^{-1}) Heteroaggregation ($k_{hetero\text{-}agg}$= 2.3 × 10^{-7} s^{-1}) Advection (k_{adv}= 4.6 × 10^{-8} s^{-1}) Photodegradation ($k_{photodeg}$= 1.3 × 10^{-7} s^{-1})	27.2	93	30.7	7.78E+02	(Deng et al., 2017b)
SWCNT	Calculated using substance specific partitioning coefficients	S1) 143 S2) matter of days	S1) 100 S2) 98	S1) 200 S2) 200	S1) 29000 S2) 3700	(Eckelman et al., 2012)
Nano-TiO_2	Dissolution Aggregation	0.633 (free form) 44.8 (aggregated form)	*not mentioned*	26.9 (9.4–26.9)	1550 (free form)	(Ettrup et al., 2017)
nAg	Calculated using substance specific partitioning coefficients	S1) 30 S2) 130	S1) 60 S2) 80	S1) 13497 S2) 281144	S1) 2.43E+05 S2) 2.92E+07	(Garvey et al., 2019)
Nano-TiO_2	Calculated using substance specific partitioning coefficients	S1) 0.053 S2) 1	S1) 100 S2) 100	S1) 79 S2) 1180	S1) 4 S2) 1180	(Garvey et al., 2019)

SWCNT	Calculated using substance specific partitioning coefficients	S1) 10 S2) 143	S1) 100 S2) 100	S1) 260 S2) 288	S1) 2600 S2) 41184	(Garvey et al., 2019)
C_{60}	Calculated using substance specific partitioning coefficients	S1) 10 S2) 143	S1) 100 S2) 100	S1) 91 S2) 161	S1) 910 S2) 23023	(Garvey et al., 2019)
nAg	Assumed due to many unknowns	1	neglected	8576	8.57E+03	(Miseljic and Olsen, 2014)
Nano-TiO_2	Assumed due to many unknowns	1	neglected	26.1	2.61E+01	(Miseljic and Olsen, 2014)
nCu	Sedimentation Advection Dissolution	1.15	100	5185	5.96E+03	(Pu et al., 2016)
nAg	Sedimentation Advection (k_{adv}= 8.1 × 10^{-9} s^{-1}) Dissolution (k_{diss}=3.42 × 10^{-6} s^{-1})	1.36 (3.86E-03 – 3.38E+00)	100	14502	1.98E+04	(Pu, 2017)
Al_2O_3-NP	Sedimentation Advection (k_{adv}= 8.1 × 10^{-9} s^{-1})	2.28 (3.87E-03 – 1.28E+03)	100	53.083	1.21E+02	(Pu, 2017)
Au-NP	Sedimentation Advection (k_{adv}= 8.1 × 10^{-9} s^{-1})	2.28 (3.87E-03 – 1.18E+03)	100	80.7	1.84E+02	(Pu, 2017)
C_{60}	Sedimentation Advection (k_{adv}= 8.1 × 10^{-9} s^{-1})	2.28 (3.87E-03 – 1.33E+03)	100	544	1.24E+03	(Pu, 2017)
CeO_2-NP	Sedimentation Advection (k_{adv}= 8.1 × 10^{-9} s^{-1})	2.28 (3.87E-03 – 1.24E+03)	100	139	3.18E+02	(Pu, 2017)
nCu	Sedimentation Advection (k_{adv}= 8.1 × 10^{-9} s^{-1}) Dissolution (k_{diss}=5.5 × 10^{-7} s^{-1})	2.06 (3.87E-03 – 2.07E+01)	100	8999	1.85E+04	(Pu, 2017)

nCuO	Sedimentation Advection (k_{adv}= 8.1 × 10^{-9} s^{-1}) Dissolution (k_{diss}=3.87 × 10^{-7} s^{-1})	2.12 (1.37E-01 – 2.92E+01)	100	223	4.74E+02	(Pu, 2017)
Fe_2O_3-NP	Sedimentation Advection (k_{adv}= 8.1 × 10^{-9} s^{-1})	2.28 (3.86E-03 – 1.26E+03)	100	228	5.20E+02	(Pu, 2017)
Fe_3O_4-NP	Sedimentation Advection (k_{adv}= 8.1 × 10^{-9} s^{-1})	2.28 (3.87E-03 – 1.27E+03)	100	21739	4.96E+04	(Pu, 2017)
NiO-NP	Sedimentation Advection (k_{adv}= 8.1 × 10^{-9} s^{-1}) Dissolution (k_{diss}=2.18 × 10^{-7} s^{-1})	2.19 (3.87E-03 – 5.09E+01)	100	14.2	3.10E+01	(Pu, 2017)
Pt-NP	Sedimentation Advection (k_{adv}= 8.1 × 10^{-9} s^{-1})	2.28 (3.86E-03 – 1.17E+03)	100	126	2.88E+02	(Pu, 2017)
SiO_2-NP	Sedimentation Advection (k_{adv}= 8.1 × 10^{-9} s^{-1}) Dissolution (k_{diss}=3.79 × 10^{-6} s^{-1})	1.31 (3.86E-03 – 3.05E+00)	100	27.8	3.62E+01	(Pu, 2017)
Nano-TiO_2	Sedimentation Advection (k_{adv}= 8.1 × 10^{-9} s^{-1})	2.28 (3.87E-03 – 1.27E+03)	100	56.7	1.29E+02	(Pu, 2017)
ZnO-NP	Sedimentation Advection (k_{adv}= 8.1 × 10^{-9} s^{-1}) Dissolution (k_{diss}=5.12 × 10^{-7} s^{-1})	2.07 (3.87E-03 – 2.22E+01)	100	2863	5.94E+03	(Pu, 2017)
SWCNT	Calculated using substance specific partitioning coefficients	29	6.5E-04	650	1.25E-01	(Rodriguez-Garcia et al., 2014)

MWCNT	Calculated using substance specific partitioning coefficients	92	100	8	7.40E+02	(Rodriguez-Garcia et al., 2014)
nCu	Calculated using substance specific partitioning coefficients	37	33	4500	5.52E+04	(Rodriguez-Garcia et al., 2014)
Nano-TiO_2	Sedimentation Heteroaggregation Advection	0.053	100	32.1	2.81E+01	(Salieri et al., 2015)

Dissolution

$$4Ag_{(s)} + O_{2\,(aq)} \rightarrow 2Ag_2O_{(s)} \qquad (S1)$$

$$Ag_2O_{(s)} + 2H^+{}_{(aq)} \rightarrow 2Ag^+{}_{(aq)} + H_2O_{(l)} \qquad (S2)$$

$$2Ag_{(s)} + \frac{1}{2}O_{2\,(aq)} + 2H^+{}_{(aq)} \rightarrow 2Ag^+{}_{(aq)} + H_2O_{(l)} \qquad (S3)$$

The second method for k_{diss} calculation is using modified version of the solubility equilibrium (i.e. Ostwald-Freundlich relation) as presented in equations (S4) and (S5), which enables calculating size-dependent dissolution rates (Axson et al., 2015; Doody et al., 2016; Johnston et al., 2019; Ma et al., 2012). It is hypothesized that the amount of dissolved nAg per unit time is proportional with the surface area of nAg (Molleman and Hiemstra, 2017; Quik et al., 2011) as

$$\frac{dM}{dt} = -k_{diss} * S_{nAg} * A \qquad (S4)$$

$$S_{nAg} = S_{bulk} * \exp\left(2 * \gamma * \frac{V_m}{R * T * r_{nAg}}\right) \qquad (S5)$$

where M is the dissolved mass of nAg (kg), t is time (s), S_{nAg} is the solubility of nAg (kg/m^3), A is the surface area of nAg (m^2), S_{bulk} is the solubility of bulk silver (kg/m^3), γ is the surface tension of nAg (typically 1 for nAg, J/m^2), V_m is the molar volume of nAg (m^3/mol), R is the gas constant (J/mol.K), T is the temperature (K) and r_{nAg} is the radius of nAg (m). Ma et al. calculated the k_{diss} for PVP coated nAg as 5.07×10^{-5} s^{-1} using this method (Ma et al., 2012). Different from the previously explained methods, Dale et al. compiled a list of model parameters for nAg transformation where they included a range for k_{diss} based on the level of dissolved oxygen in freshwaters from 1.3×10^{-8} d^{-1} (mg O_2/m^3)$^{-1}$ to 5.1×10^{-4} d^{-1} (mg O_2/m^3)$^{-1}$ with a nominal value of 8.5×10^{-6} d^{-1} (mg O_2/m^3)$^{-1}$ (Dale et al., 2015; Levard et al., 2012; Liu et al., 2010).

Hetero-aggregation

$$k_{het-agg} = k_{coll} * \alpha_{het-agg} * C_{SPM} \qquad (S6)$$

where $\alpha_{het-agg}$ is aggregation efficiency, C_{SPM} is suspended particulate matter concentration (1/m^3) and k_{coll} is the collision rate (m^3/s). C_{SPM} needs to be calculated using equation (S7) as

$$C_{SPM} = \frac{C_{mass,\,SPM}}{\frac{4}{3} * \rho_{SPM} * \pi * \left(\frac{d_{SPM}}{2}\right)^3} \qquad (S7)$$

where $C_{mass,\,SPM}$ is the mass concentration of suspended particulate matter in water (kg/m^3), ρ_{SPM} is the density of suspended particulate matter (kg/m^3) and d_{SPM} is the diameter of the suspended particulate matter in water (m). Another component of equation (S6), the collision rate, can be calculated using equation (S8).

$$k_{coll} = \frac{2k_B T_{water}}{3\mu_{water}} * \frac{(r_{nAg} + r_{SPM})^2}{r_{nAg} * r_{SPM}} + \frac{4}{3}G(r_{nAg} + r_{SPM})^3 + \pi(r_{nAg} + r_{SPM})^2 * \left|v_{set}^{nAg} - v_{set}^{SPM}\right| \qquad (S8)$$

where k_B is Boltzmann constant (JK^{-1}), T_{water} is the temperature of the water (K), μ_{water} is the dynamic viscosity of water (Ns/m^2), r_{nAg} is the radius of nAg (m), r_{SPM} is the radius of suspended particulate matter (m), G is the shear rate of the water (1/s), v_{set}^{nAg} is the settling velocity of nAg (m/s) and v_{set}^{SPM} is the settling velocity of suspended particulate matter (m/s). Equations (S9) and (S10) are used to calculate the settling velocities of nAg and SPM to be used in the collision rate calculation.

$$v_{set}^{nAg} = \frac{2}{9} * \frac{\rho_{nAg} - \rho_{water}}{\mu_{water}} * g * r_{nAg}^2 \qquad (S9)$$

$$v_{set}^{SPM} = \frac{2}{9} * \frac{\rho_{SPM} - \rho_{water}}{\mu_{water}} * g * r_{SPM}^2 \qquad (S10)$$

where ρ_{nAg} is the density of nAg (kg/m^3), ρ_{water} is the density of water (kg/m^3), μ_{water} is the dynamic viscosity of water (Ns/m^2), g is is the gravitational acceleration on earth (m/s^2), r_{nAg} is the radius of nAg (m), ρ_{SPM} is the density of suspended particulate matter (kg/m^3) and r_{SPM} is the radius of suspended particulate matter (m).

Sedimentation

Scenario 2

$$k_{sed}^{'} = k_{sed}^{nAg} + k_{agg-sed} + k_{att-sed} \qquad (S11)$$

where k_{sed}^{nAg} is the sedimentation rate constant (s^{-1}), $k_{agg-sed}$ is the minimum value of either pseudo-sedimentation rate constant for homo-aggregated nAg or the homo-aggregation rate constant as expressed in equation (S12) (s^{-1}) and $k_{att-sed}$ is the minimum value of either pseudo-sedimentation rate constant for hetero-aggregated (i.e. attached) nAg or the hetero-aggregation (i.e. attachment) rate constant as expressed in equation (S13) (s^{-1}).

$$k_{agg-sed} = minimum\left(k_{homo-agg}, k_{ps-homo-agg}\right) \qquad (S12)$$

where k_{agg} is the aggregation rate constant and k_{ps-agg} is the pseudo-sedimentation rate constant for aggregated nAg. In the current study, homo-aggregation is neglected, therefore this component is not calculated.

$$k_{att-sed} = minimum\left(k_{het-agg}, k_{ps-het-agg}\right) \qquad (S13)$$

where $k_{het-agg}$ is the attachment rate constant and $k_{ps-het-agg}$ is the pseudo-sedimentation rate constant for attached nAg.

$$k_{sed}^{nAg} = \frac{v_{set}^{nAg}}{h_w} \qquad (S14)$$

where v_{set}^{nAg} is the settling velocity of nAg as expressed in equation (S9) (m/s) and h_w is the depth of the water compartment (m).

$$k_{ps-het-agg} = \frac{v_{set}^{SPM}}{h_w} \qquad (S15)$$

where v_{set}^{SPM} is the settling velocity of suspended particulate matter as expressed in equation (S10) (m/s) and h_w is the depth of the water compartment (m).

Table S4. Calculated parameters based on the values presented in Tables S2-S3 (shaded values are used in FF calculation for the respective scenarios)

Parameter	**Symbol**	**Unit**	**Value (Scenario 1)**	**Value (Scenario 2)**
Dissolution rate constant	k_{diss}	s^{-1}	3.15×10^{-7}	3.15×10^{-7}
Hetero aggregation rate constant	$k_{het-agg}$	s^{-1}	3.44×10^{-5}	-
Concentration of SPM	C_{SPM}	$1/m^3$	2.88×10^{13}	2.88×10^{13}
Collision rate	k_{coll}	m^3/s	9.95×10^{-17}	9.95×10^{-17}
Settling velocity of nAg	v_{set}^{nAg}	m/s	1.31×10^{-8}	1.31×10^{-8}
Settling velocity of SPM	v_{set}^{SPM}	m/s	7.29×10^{-7}	7.29×10^{-7}
Sedimentation rate constant	k_{sed}	s^{-1}	1.09×10^{-8}	6.19×10^{-7}
Advection rate constant	k_{adv}	s^{-1}	2.05×10^{-8}	2.05×10^{-8}
Removal rate constant for freshwater	$k_{w,w}$	s^{-1}	3.48×10^{-5}	9.54×10^{-7}
Fate factor	FF	days	0.33	12

Table S5. List of characterization factors calculated in the current study and the literature values

Reference	Scenarios	XF (%)	FF (days)	EF (PAF.m^3/kg)	CF (PAF.m^3.day/kg or CTUe/kg)
(Garvey et al., 2019)	S1	60	30	1.35×10^4	2.43×10^5
	S2	80	130	2.81×10^5	2.92×10^7
(Pu, 2017)	-	100	1.36	1.45×10^4	1.97×10^4
(Miseljic and Olsen, 2014)	-	100	1	8.58×10^3	8.58×10^3
This study	S1 – Optimistic (regardless of coating)	100	0.33	8.04×10^3	2.67×10^3
	S1 – Skeptical (regardless of coating)	100	0.33	1.47×10^4	4.88×10^3
	S2 – Optimistic (regardless of coating)	100	12.13	8.04×10^3	9.74×10^4
	S2 – Skeptical (regardless of coating)	100	12.13	1.47×10^4	1.78×10^5
	S1 – Optimistic (PVP coated)	100	0.33	6.58×10^3	2.19×10^3
	S1 – Skeptical (PVP coated)	100	0.33	1.93×10^4	6.42×10^3
	S2 – Optimistic (PVP coated)	100	12.13	6.58×10^3	7.98×10^4
	S2 – Skeptical (PVP coated)	100	12.13	1.93×10^4	2.34×10^5
USEtox spreadsheet	For ionic silver Ag (I)	41.2	18.1	2.60×10^4	1.94×10^5

Table S6. Scenario 1: sensitivity factors (SF) based on 20% change of inputs on the rate constants and fate factor. Reported numbers are SFs, where red cells indicate sensitive inputs.

	d_{nAg}	d_{SPM}	ρ_{nAg}	$\alpha_{het-agg}$	$C_{mass,SPM}$	C_0	C_{ions}	ρ_{SPM}
$k_{het-agg}$	-1.67E-01	-4.04E-01	-5.50E-05	1.67E-01	1.67E-01	0.00E+00	0.00E+00	-1.91E-01
k_{sed}	3.06E-01	0.00E+00	1.81E-01	0.00E+00	0.00E+00	0.00E+00	0.00E+00	0.00E+00
k_{diss}	0.00E+00	0.00E+00	0.00E+00	0.00E+00	0.00E+00	-2.06E-01	1.71E-01	0.00E+00
k_{adv}	0.00E+00	0.00E+00	0.00E+00	0.00E+00	0.00E+00	0.00E+00	0.00E+00	0.00E+00
$k_{w,w}$	-1.65E-01	-3.98E-01	1.51E-05	1.65E-01	1.65E-01	-1.55E-03	1.87E-03	-1.89E-01
FF	1.41E-01	2.85E-01	-1.51E-05	-1.98E-01	-1.98E-01	1.54E-03	-1.87E-03	1.59E-01

Table S7. Scenario 1: sensitivity factors (SF) based on 20% change of rate constants on fate factor. Reported numbers are SFs, where red cells indicate sensitive inputs.

	$k_{het-agg}$	k_{sed}	k_{diss}	k_{adv}
$k_{w,w}$	1.65E-01	6.29E-05	1.81E-03	-1.18E-04
FF	-1.98E-01	-6.29E-05	-1.81E-03	-1.18E-04

Table S8. Scenario 2: sensitivity factors (SF) based on 20% change of inputs on the rate constants and fate factor. Reported numbers are SFs, where red cells indicate sensitive inputs.

	d_{nAg}	d_{SPM}	ρ_{nAg}	$\alpha_{het-agg}$	$C_{mass,SPM}$	C_0	C_{ions}	ρ_{SPM}
k_{sed}	7.72E-03	3.02E-01	3.89E-03	0.00E+00	0.00E+00	0.00E+00	0.00E+00	3.51E-01
k_{diss}	0.00E+00	0.00E+00	0.00E+00	0.00E+00	0.00E+00	-2.06E-01	1.71E-01	0.00E+00
k_{adv}	0.00E+00	0.00E+00	0.00E+00	0.00E+00	0.00E+00	0.00E+00	0.00E+00	0.00E+00
$k_{w,w}$	5.02E-03	2.19E-01	2.53E-03	0.00E+00	0.00E+00	-5.96E-02	6.39E-02	2.60E-01
FF	-5.05E-03	-2.80E-01	-2.53E-03	0.00E+00	0.00E+00	5.63E-02	-6.82E-02	-3.51E-01

Table S9. Scenario 2: sensitivity factors (SF) based on 20% change of rate constants on fate factor. Reported numbers are SFs, where red cells indicate sensitive inputs.

	k_{sed}	k_{diss}	k_{adv}
$k_{w,w}$	1.15E-01	6.19E-02	4.28E-03
FF	-1.30E-01	-6.60E-02	-4.30E-03

References

Axson, J.L., Stark, D.I., Bondy, A.L., Capracotta, S.S., Maynard, A.D., Philbert, M.A., Bergin, I.L., Ault, A.P., 2015. Rapid Kinetics of Size and pH-Dependent Dissolution and Aggregation of Silver Nanoparticles in Simulated Gastric Fluid. J. Phys. Chem. C 119, 20632–20641. https://doi.org/10.1021/acs.jpcc.5b03634

Baun, A., Sayre, P., Steinhäuser, K.G., Rose, J., 2017. Regulatory relevant and reliable methods and data for determining the environmental fate of manufactured nanomaterials. NanoImpact 8, 1–10. https://doi.org/10.1016/j.impact.2017.06.004

Dale, A.L., Casman, E.A., Lowry, G.V., Lead, J.R., Viparelli, E., Baalousha, M., 2015. Modeling Nanomaterial Environmental Fate in Aquatic Systems. Environ. Sci. Technol. 49, 2587–2593. https://doi.org/10.1021/es505076w

Dale, A.L., Lowry, G.V., Casman, E.A., 2013. Modeling Nanosilver Transformations in Freshwater Sediments. Environ. Sci. Technol. 47, 12920–12928. https://doi.org/10.1021/es402341t

Deng, Y., Li, J., Li, T., Zhang, J., Yang, F., Yuan, C., 2017a. Life cycle assessment of high capacity molybdenum disulfide lithium-ion battery for electric vehicles. Energy 123, 77–88. https://doi.org/10.1016/j.energy.2017.01.096

Deng, Y., Li, J., Qiu, M., Yang, F., Zhang, J., Yuan, C., 2017b. Deriving characterization factors on freshwater ecotoxicity of graphene oxide nanomaterial for life cycle impact assessment. Int J Life Cycle Assess 22, 222–236. https://doi.org/10.1007/s11367-016-1151-4

Doody, M.A., Wang, D., Bais, H.P., Jin, Y., 2016. Differential antimicrobial activity of silver nanoparticles to bacteria Bacillus subtilis and Escherichia coli, and toxicity to crop plant Zea mays and beneficial B. subtilis-inoculated Z. mays. J Nanopart Res 18, 290. https://doi.org/10.1007/s11051-016-3602-z

Eckelman, M.J., Mauter, M.S., Isaacs, J.A., Elimelech, M., 2012. New Perspectives on Nanomaterial Aquatic Ecotoxicity: Production Impacts Exceed Direct Exposure Impacts for Carbon Nanotoubes. Environ. Sci. Technol. 46, 2902–2910. https://doi.org/10.1021/es203409a

Espinasse, B.P., Geitner, N.K., Schierz, A., Therezien, M., Richardson, C.J., Lowry, G.V., Ferguson, L., Wiesner, M.R., 2018. Comparative Persistence of Engineered Nanoparticles in a Complex Aquatic Ecosystem. Environ. Sci. Technol. 52, 4072–4078. https://doi.org/10.1021/acs.est.7b06142

Ettrup, K., Kounina, A., Hansen, S.F., Meesters, J.A.J., Vea, E.B., Laurent, A., 2017. Development of Comparative Toxicity Potentials of TiO2 Nanoparticles for Use in Life Cycle Assessment. Environ. Sci. Technol. 51, 4027–4037. https://doi.org/10.1021/acs.est.6b05049

Fantke, P., Bijster, M., Guignard, C., Hauschild, M.Z., Huijbregts, M., Jolliet, O., Kounina, A., Magaud, V., Margni, M., McKone, T.E., Posthuma, L., Rosenbaum, R.K., Van De Meent, D., Van Zelm, R., 2017. USEtox® 2.0 Documentation (Version 1.00). https://doi.org/10.11581/DTU:00000011

Furtado, L.M., Norman, B.C., Xenopoulos, M.A., Frost, P.C., Metcalfe, C.D., Hintelmann, H., 2015. Environmental Fate of Silver Nanoparticles in Boreal Lake Ecosystems. Environ. Sci. Technol. 49, 8441–8450. https://doi.org/10.1021/acs.est.5b01116

Garvey, T., Moore, E.A., Babbitt, C.W., Gaustad, G., 2019. Comparing ecotoxicity risks for nanomaterial production and release under uncertainty. Clean Technol Environ Policy 21, 229–242. https://doi.org/10.1007/s10098-018-1648-6

Geitner, N.K., Bossa, N., Wiesner, M.R., 2019. Formulation and Validation of a Functional Assay-Driven Model of Nanoparticle Aquatic Transport. Environ. Sci. Technol. 53, 3104–3109. https://doi.org/10.1021/acs.est.8b06283

Geitner, N.K., O'Brien, N.J., Turner, A.A., Cummins, E.J., Wiesner, M.R., 2017. Measuring Nanoparticle Attachment Efficiency in Complex Systems. Environ. Sci. Technol. 51, 13288–13294. https://doi.org/10.1021/acs.est.7b04612

Hartmann, N.B., Skjolding, L.M., Hansen, S.F., Kjølholt, J., Gottschalck, F., Baun, A., 2014. Environmental fate and behaviour of nanomaterials - new knowledge on important transformation processes (No. 1594). Danish Environmental Protection Agency, Copenhagen, Denmark.

Johnston, K.A., Stabryla, L.M., Gilbertson, L.M., Millstone, J.E., 2019. Emerging investigator series: connecting concepts of coinage metal stability across length scales. Environ. Sci.: Nano 6, 2674–2696. https://doi.org/10.1039/C9EN00407F

Kounina, A., Margni, M., Shaked, S., Bulle, C., Jolliet, O., 2014. Spatial analysis of toxic emissions in LCA: A sub-continental nested USEtox model with freshwater archetypes. Environment International 69, 67–89. https://doi.org/10.1016/j.envint.2014.04.004

Lamon, L., Asturiol, D., Vilchez, A., Ruperez-Illescas, R., Cabellos, J., Richarz, A., Worth, A., 2019. Computational models for the assessment of manufactured nanomaterials: Development of model reporting standards and mapping of the model landscape. Computational Toxicology 9, 143–151. https://doi.org/10.1016/j.comtox.2018.12.002

Levard, C., Hotze, E.M., Lowry, G.V., Brown, G.E., 2012. Environmental Transformations of Silver Nanoparticles: Impact on Stability and Toxicity. Environ. Sci. Technol. 46, 6900–6914. https://doi.org/10.1021/es2037405

Liu, J., Sonshine, D.A., Shervani, S., Hurt, R.H., 2010. Controlled Release of Biologically Active Silver from Nanosilver Surfaces. ACS Nano 4, 6903–6913. https://doi.org/10.1021/nn102272n

Ma, R., Levard, C., Marinakos, S.M., Cheng, Y., Liu, J., Michel, F.M., Brown, G.E., Lowry, G.V., 2012. Size-Controlled Dissolution of Organic-Coated Silver Nanoparticles. Environ. Sci. Technol. 46, 752–759. https://doi.org/10.1021/es201686j

Maiga, D.T., Nyoni, H., Mamba, B.B., Msagati, T.A.M., 2020. The role and influence of hydrogeochemistry in the behaviour and fate of silver nanoparticles in freshwater systems. SN Appl. Sci. 2, 326. https://doi.org/10.1007/s42452-020-2130-8

Meesters, J.A.J., Koelmans, A.A., Quik, J.T.K., Hendriks, A.J., van de Meent, D., 2014. Multimedia Modeling of Engineered Nanoparticles with SimpleBox4nano: Model Definition and Evaluation. Environ. Sci. Technol. 48, 5726–5736. https://doi.org/10.1021/es500548h

Miseljic, M., Olsen, S.I., 2014. Life-cycle assessment of engineered nanomaterials: a literature review of assessment status. J Nanopart Res 16, 2427. https://doi.org/10.1007/s11051-014-2427-x

Molleman, B., Hiemstra, T., 2017. Time, pH, and size dependency of silver nanoparticle dissolution: the road to equilibrium. Environ. Sci.: Nano 4, 1314–1327. https://doi.org/10.1039/C6EN00564K

Peijnenburg, W.J.G.M., Baalousha, M., Chen, J., Chaudry, Q., Von der kammer, F., Kuhlbusch, T.A.J., Lead, J., Nickel, C., Quik, J.T.K., Renker, M., Wang, Z., Koelmans, A.A., 2015. A Review of the Properties and Processes Determining the Fate of Engineered Nanomaterials in the Aquatic Environment. Critical Reviews in Environmental Science and Technology 45, 2084–2134. https://doi.org/10.1080/10643389.2015.1010430

Peng, C., Zhang, W., Gao, H., Li, Y., Tong, X., Li, K., Zhu, X., Wang, Y., Chen, Y., 2017. Behavior and Potential Impacts of Metal-Based Engineered Nanoparticles in Aquatic Environments. Nanomaterials 7, 21. https://doi.org/10.3390/nano7010021

Praetorius, A., Scheringer, M., Hungerbühler, K., 2012. Development of Environmental Fate Models for Engineered Nanoparticles—A Case Study of TiO_2 Nanoparticles in the Rhine River. Environ. Sci. Technol. 46, 6705–6713. https://doi.org/10.1021/es204530n

Pu, Y., 2017. Toxicity assessment of engineered nanoparticles (PhD). UniversitédeTechnologie de Troyes.

Pu, Y., Tang, F., Adam, P.-M., Laratte, B., Ionescu, R.E., 2016. Fate and Characterization Factors of Nanoparticles in Seventeen Subcontinental Freshwaters: A Case Study on Copper Nanoparticles. Environ. Sci. Technol. 50, 9370–9379. https://doi.org/10.1021/acs.est.5b06300

Quik, J.T.K., 2013. Fate of nanoparticles in the aquatic environment: removal of engineered nanomaterials from the water phase under environmental conditions. Radboud University, Nijmegen, The Netherlands.

Quik, J.T.K., Vonk, J.A., Hansen, S.F., Baun, A., Van De Meent, D., 2011. How to assess exposure of aquatic organisms to manufactured nanoparticles? Environment International 37, 1068–1077. https://doi.org/10.1016/j.envint.2011.01.015

Rodriguez-Garcia, G., Zimmermann, B., Weil, M., 2014. Nanotoxicity and Life Cycle Assessment: First attempt towards the determination of characterization factors for carbon nanotubes. IOP Conference Series: Materials Science and Engineering 64, 012029. https://doi.org/10.1088/1757-899X/64/1/012029

Rosenbaum, R.K., Bachmann, T.M., Gold, L.S., Huijbregts, M.A.J., Jolliet, O., Juraske, R., Koehler, A., Larsen, H.F., MacLeod, M., Margni, M., McKone, T.E., Payet, J., Schuhmacher, M., van de Meent, D., Hauschild, M.Z., 2008. USEtox—the UNEP-SETAC toxicity model: recommended characterisation factors for human toxicity and freshwater ecotoxicity in life cycle impact assessment. Int J Life Cycle Assess 13, 532–546. https://doi.org/10.1007/s11367-008-0038-4

Salieri, B., Righi, S., Pasteris, A., Olsen, S.I., 2015. Freshwater ecotoxicity characterisation factor for metal oxide nanoparticles: A case study on titanium dioxide nanoparticle. Science of The Total Environment 505, 494–502. https://doi.org/10.1016/j.scitotenv.2014.09.107

Stegemeier, J.P., Colman, B.P., Schwab, F., Wiesner, M.R., Lowry, G.V., 2017. Uptake and Distribution of Silver in the Aquatic Plant *Landoltia punctata* (Duckweed) Exposed to Silver and Silver Sulfide Nanoparticles. Environ. Sci. Technol. 51, 4936–4943. https://doi.org/10.1021/acs.est.6b06491

Temizel-Sekeryan, S., Hicks, A.L., 2020. Emerging investigator series: Calculating size- and coating- dependent effect factors for silver nanoparticles to inform characterization factor development for usage in life cycle assessment. Environ. Sci.: Nano 10.1039.D0EN00675K. https://doi.org/10.1039/D0EN00675K

Tortella, G.R., Rubilar, O., Durán, N., Diez, M.C., Martínez, M., Parada, J., Seabra, A.B., 2020. Silver nanoparticles: Toxicity in model organisms as an overview of its hazard for human health and the environment. Journal of Hazardous Materials 390, 121974. https://doi.org/10.1016/j.jhazmat.2019.121974

Westerhoff, P., Nowack, B., 2013. Searching for Global Descriptors of Engineered Nanomaterial Fate and Transport in the Environment. Acc. Chem. Res. 46, 844–853. https://doi.org/10.1021/ar300030n